ELSEVIER

PII: S0144-8617(97)00231-2

Carbohydrate Polymers **35** (1998) 55–63

0144-8617/98/$19.00+0.00

Rheological properties of guar galactomannan and rice starch mixtures. II. Creep measurements[1]

Phillippa Rayment*, Simon B. Ross-Murphy, Peter R. Ellis

Biopolymers Group, Division of Life Sciences, King's College London, Campden Hill Road, London W8 7AH, UK

(Received 14 March 1997; revised 7 July 1997; accepted 21 July 1997)

The effect of particulate inclusions, or 'fillers', on the rheological properties of a typical polysaccharide entanglement solution (guar galactomannan/water) have been studied. Earlier steady shear experiments have shown an apparent upswing of the viscosity–shear rate profiles at low shear rates, with higher filler concentrations (Rayment *et al.*, 1995). In creep experiments, a low constant stress is applied to the sample.

In the present paper, the creep experimental data have been compared to the steady shear flow behaviour fitted by the yield stress modified Cross equation (introduced in Part I of this series).

The apparent zero-shear viscosity and yield stress parameters have been constrained in a number of ways in the model to establish the effect of these parameters on the modified Cross model. Although the creep data appears to alter the precision of the modified Cross equation, due to the low shear rates accessed, the apparent upswing of the steady shear data at low shear rates appear to be supported by the data described in this paper. This lends further credibility to the scaled filler models introduced previously.

INTRODUCTION

Guar galactomannan is a water-soluble polysaccharide with an essentially linear β-D-(1/4)-mannan backbone and irregularly substituted, uncharged α-D-(1/6)-linked galactose side groups (Dea and Morrison, 1975). In the present work, aqueous solutions of guar gum, well recognised to be model entanglement network systems (Doublier and Launay, 1981; Robinson *et al.*, 1982; Richardson and Ross-Murphy, 1987), were measured in a step stress (creep) test. A creep test is a steady transient test in which a known stress (τ_0) is applied to a material and the resulting deformation with time (γ_t) is measured. This can be investigated by monitoring the creep compliance parameter $J(t)$, which is the resulting strain divided by the applied stress. The time (t) is approximately equivalent to low frequencies ($t \approx 2\pi/\omega$) in an oscillatory experiment and therefore creep experiments are appropriate for determining viscoelastic constants with long relaxation times.

The Cross equation (Eq. (1)) is often used to describe the shear-thinning behaviour of guar gum dispersions (Cross, 1965) and has been used in many scientific publications (Sharman *et al.*, 1978; Doublier and Launay, 1981; Rayment *et al.*, 1995).

$$\eta = \eta_\infty + [\eta_{0X} - \eta_\infty]/[1 + (a\dot{\gamma})^p] \quad (1)$$

where η_{0X} and η_∞ are limiting (Cross) viscosities, at zero and infinite shear rates, a and $\dot{\gamma}$ are a relaxation time and shear rate, respectively, whilst p is an exponent.

For the current study, a rice starch filler, selected for size and homogeneity of starch grain, was then added to the guar galactomannan solutions in small increments and the system was measured in creep. As the amount of filler is increased we would expect that the flow behaviour of the dispersion would begin to develop some additional features. It has been well known for some time that one of the major effects

*Corresponding author. Tel: +44 (0)171-333 4232; fax: +44(0)171-333 4082; e-mail: pip.rayment@kcl.ac.uk

[1] For Part I, see Rayment et al. (1995).

of increasing particle volume fraction is to modify the viscosity–shear rate profile (Rutgers, 1962). For filled Newtonian fluids, a more 'power law' like $\eta(\dot{\gamma})$ profile is seen, with an apparent upswing at the lowest shear rates. This has been suggested to be related to an apparent yield stress developing at lower shear rates. Consequently, in order to study the behaviour of small particles in non-Newtonian (pseudoplastic) fluids, such as polysaccharide gum solutions, the Cross equation must be modified to include a yield stress term (τ_X), converting Eq. (1) to Eq. (2).

$$\eta = \eta_\infty + [\eta_{0X} - \eta_\infty]/[1 + (a\dot{\gamma})^p] + (\tau_X/\dot{\gamma}) \quad (2)$$

An 'apparent' yield stress can then be determined by extrapolating the flow data back to zero shear rate using a mathematical model. This model has been applied in a slightly different form by other workers (Castelain *et al.*, 1986; Lapasin and Pricl, 1995).

In a creep experiment, the transducer system in the controlled stress instrument allows a constant stress to be applied to the sample and as such, lower shear rates may be accessed. This should extend the information obtained in steady shear measurements of this guar galactomannan/rice starch system (Rayment *et al.*, 1995) to much lower shear rate regimes. In general, creep compliance studies can provide an insight into the rheological behaviour of such systems, practically in their undisturbed state.

MATERIALS AND METHODS

A guar gum sample (Meyprogat 90) was kindly provided by Meyhall Chemicals, A.G., Rhône Poulenc Group, Switzerland. The sample was isolated and purified as described by Rayment *et al.* (1995). The relative proportions of galactose and mannose and the molecular weight were determined by methods published in Part I of this series (Rayment *et al.*, 1995).

Guar gum solutions were prepared by dissolving a known weight of the dried material in distilled water to give nominal galactomannan concentrations of 1, 2 and 3% (w/w), respectively. The solutions were then heated to 80°C for 5 min followed by stirring at room temperature overnight to ensure complete hydration of the polymer. Preliminary experiments were carried out using solutions of unpurified Meyprogat 90 samples, prepared in the same way as the purified samples.

An insoluble, cosmetic rice starch sample was kindly provided by Cairn Foods (Remy Industries, S.A., Belgium). The rice starch was then added to the guar solutions so that the galactomannan concentration in the aqueous medium was kept constant while the starch filler concentration was varied from 0 to 41% (w/w). The density, maximum packing fraction (ϕ_{max}) and the particle size of the rice starch particles were determined as described by Rayment *et al.* (1995). Creep measurements were carried out using a filled 1% guar galactomannan solution only because earlier work had clearly demonstrated that in this range, the reduced (apparent) viscosity could be scaled independent of the polymer concentration.

Steady shear measurements

Experiments were performed at 25°C using a Rheometrics Fluids Spectrometer (RFSII, Rheometric Scientific Ltd., Epsom, Surrey, UK) with a cone and plate configuration and a cone angle of 0.02 radians. The transducer system measured torque in a dual range of 0.002–10 g. cm and 0.02–100 g. cm, which corresponded to a stress range of 0.006–300 Pa with this geometry. Problems encountered with drying of the samples were reduced by applying a thin layer of a high viscosity paraffin oil to the exposed surface and the use of a solvent trap. Steady shear measurements were conducted at shear rates of 0.05–1000 s^{-1}, with a reduction in rate necessary at the higher filler concentrations.

For steady shear measurements it is obligatory to employ cone and plate geometry since the shear rate approaches constancy throughout the sample. However, the truncation of the cone tip is very small ($\approx$ 50 μm) and the particle size should be $< \approx$ 1/5 of the gap truncation. Rice starch has the smallest particle size of commercial starches (6–10 μm) and, as such, was used in this case. Further experimental details are listed in Part I of this series (Rayment *et al.*, 1995).

Creep (step shear) measurements

Experiments were performed at 25°C using a Rheometrics Dynamic Stress Rheometer (DSR-200, Rheometric Scientific Ltd., Epsom, Surrey, UK) with, initially, a 25 mm diameter and 1 mm gap, parallel plate configuration and then, a 40 mm diameter and 0.04 rad cone and plate geometry. The transducer system measured torque in the range 0.01–200 g. cm. The temperature was controlled by a Neslab RTE-111 water bath and the temperature of the sample monitored using a thermocouple mounted in the bottom plate. Problems encountered with drying of the samples were again reduced by applying a thin layer of a high viscosity paraffin oil to the exposed surface and the use of a solvent trap. This consisted of a ring of cotton wool soaked in distilled water placed on the edge of the lower plate. However, these problems became progressively more severe as the filler phase volume was increased and therefore, in this configuration, we were unable to investigate samples with filler concentrations above 33% (w/w) in creep.

The step stress (creep) test is a steady transient test in which the total time of the experiment is divided into different time and/or stress zones. The test thus allows a constant stress to be applied for a selected time period and a number of selected data points to be taken in each of up to eight zones. The experiment is divided into creep and recovery phases. During the creep phase a command stress

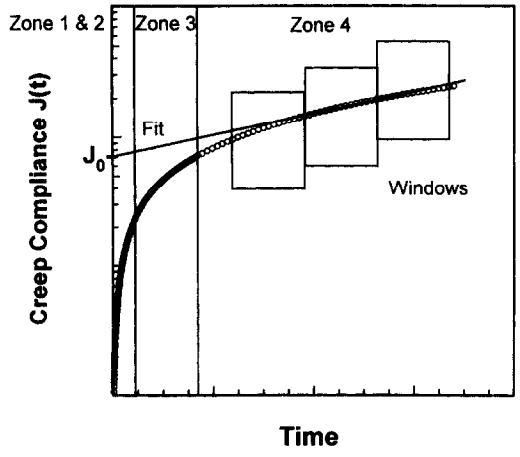

Fig. 1. Graph showing data collection set-up in creep experiment. Vertical lines indicate division of experiment into four zones. The curve is divided into windows of data and least squares fit to zero time represents instantaneous compliance, J_o.

is applied and the change in strain with time is monitored. During the recovery phase the stress is commanded to zero and the response of the sample to the removed load is observed. In this instance we were interested mainly in the creep phase of the experiment and therefore Fig. 1 shows the first four creep zones only, the recovery zone is not displayed. Both phases were divided into four zones with each zone lasting 450 s. The data points were collected in logarithmic collection mode with 50 data points per zone. In separate experiments the commanded stress was set to 0.5, 5.0 and 50.0 Pa, respectively, in an attempt to establish whether $J(t)$ was stress independent.

Preliminary experiments showed that reliable data, in the correct stress–shear rate regime, could be obtained when the stress was low (<30 Pa) and the time less than approximately 1200 s. Therefore, further creep experiments were conducted, in the main, at a stress of 0.1 Pa. The minimum stress which could be applied for the initial parallel plate geometry was 0.32 Pa. Therefore, to achieve a lower minimum command stress (0.059 Pa), the cone and plate geometry was employed. The experiment was divided into zones as listed in Tables 1 and 2. The first four zones were set to command the same constant stress, whilst in the fifth recovery zone the stress was set to zero. The time corresponding to the creep zone portion of the test was increased as the filler concentration was increased to allow steady state to be reached. The recovery phase was unchanged.

Results were fitted using the creep analysis software in the rheometer's proprietary software RHIOS (Version 4.3.2) as well as the modified Cross equation using Fig. P for Windows (Biosoft, Cambridge, UK). Creep analysis provides a tool to examine data in the steady state region of both creep and recovery zones. Using the 'Calculate Flow Term' pull down menu in RHIOS, it is possible to obtain a viscosity value for the steady state region of the creep portion of the step stress test. If the steady state region of the flow curve is not known, RHIOS automatically determines the steady state region prior to calculation. However, if the steady state region is known these data points may be selected before calculation. The curve is divided into windows of data which are dependent on the window size. A least squares fit is performed from *the end* of the curve working *back* to time zero (Fig. 1) and the steady state is determined as the point where the difference between the slopes of adjacent windows is less than the slope tolerance. The window size (10) and slope tolerance (10%) were selected on default settings since the manufacturers suggest this for most applications. A window size of 10 means that the data was divided into 10 windows. A larger window size therefore results in less data points per window. The line resulting from the least squares fit in the steady state window is extrapolated to zero time and the y-intercept of the fit is the instantaneous compliance, J_o. A corrected creep compliance ($J_c(t)$) is calculated. This is the creep compliance minus the viscous term. The final results obtained are J_o, $J_c(t)$ and η.

Table 1. Creep test set-up for 1% guar galactomannan/0–17% (w/w) rice starch samples

0–17% (w/w) filler	Zone				
	1	2	3	4	5
Stress (Pa)	0.1	0.1	0.1	0.1	0.0
Zone time (s)	20	80	320	1280	100
Points per zone	50	50	50	50	50

RESULTS

The soluble galactomannan content of purified guar gum was found to be 92.7 ± 2.3%. The ratio of galactose to mannose was 0.63 ± 0.025. For sample M90, and from the intrinsic viscosity, $[\eta]$, measured previously, the molecular weight was calculated to be 1.39×10^6 (Rayment et al., 1995). Solutions of 1% (w/w) are thus well above the critical concentration (C_{cr}) (0.24%) where semi-dilute viscosity behaviour is seen. The density of the rice starch was determined as 1.499 ± 0.058 gm l^{-1}. The maximum packing fraction (ϕ_{max}) of the starch powder was determined as 0.474 (47.4% w/w) and the particle size of the rice starch was found to range between 6–10 μm.

The effect of particulate inclusions on the steady shear viscosity–shear rate profile is displayed in Fig. 2 and

Table 2. Creep test set-up for 1% guar galactomanna/26–33% (w/w) rice starch samples

26–33% (w/w) filler	Zone				
	1	2	3	4	5
Stress (Pa)	0.1	0.1	0.1	0.1	0.0
Zone time (s)	60	240	960	3840	100
Points per zone	50	50	50	50	50

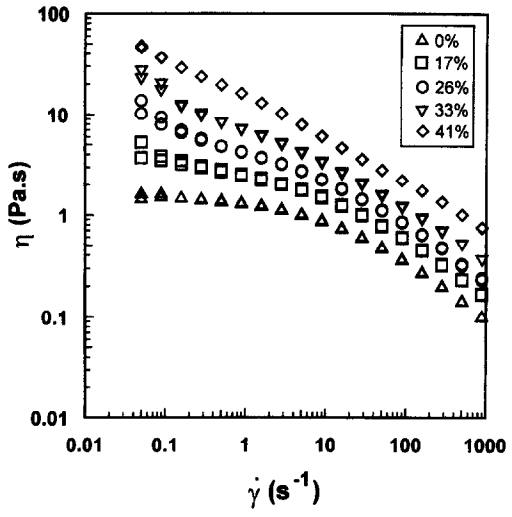

Fig. 2. Effect of increasing rice starch concentration (0–41% w/w) on the viscosity–shear rate flow curve of a 1% guar galactomannan solution. Duplicate data are displayed to show good replication of results. Figure reproduced from Rayment et al. (1995).

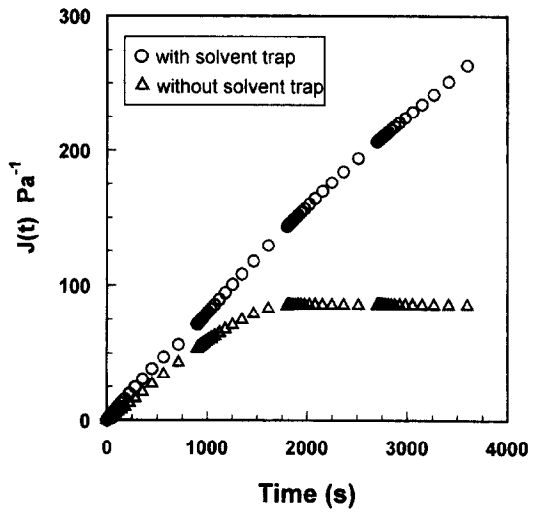

Fig. 3. Creep compliance plotted against time for a 1% guar galactomannan/25% rice starch mixture showing the effect of using a solvent trap system. Stress commanded at 0.5 Pa.

reproduced from our earlier paper (Rayment *et al.*, 1995). As the amount of filler is increased there is an increase in the steady shear viscosity above that of the pure system. The initial Newtonian flow properties of the pure system at low shear rates become more rate-dependent on increasing particulate concentration, thus generating the so-called 'power law' behaviour. From this flow data there was an indication that an extra term was required, denoted the 'yield stress', especially for the higher filler concentration regimes.

The yield stress modified Cross equation (Eq. (2)) was used to determine zero-shear viscosity (η_{0X}) and apparent yield stress (τ_X) of all the flow data. Least squares fitting to the model was accomplished using Fig. P which employs a Marquardt non-linear search algorithm. For a 2% guar galactomannan solution with 26% (w/w) rice starch filler, interpreted in terms of the modified Cross equation, the apparent yield stress was calculated as 1.52 Pa. Zero-shear viscosity and yield stress data, normalised and plotted against volume fraction, are given in Rayment *et al.* (1995).

Creep experiments

In the creep experiments, several problems were encountered with drying out of the highly filled 1% guar galactomannan solutions, due to the increased time periods necessary to access steady flow conditions. A solvent trap and plastic shield were used to reduce drying effects and the results are displayed in Fig. 3. The creep compliance of the sample tested without a solvent trap increased initially at a constant rate. However, early in the duration of the experiment the creep compliance deviated markedly from that of the sample tested with a solvent trap. At approximately 1800 s the creep compliance profile became constant indicating that flow had apparently halted.

Using the automatic steady state determination option, the RHIOS software automatically determines the steady state region of the creep compliance versus time plot (Table 3). The results showed that the shear rates accessed at an applied stress of 0.5 Pa were not much lower that those accessed in the steady shear experiments on the Fluids Spectrometer (0.05 s^{-1}). Therefore, in subsequent experiments the applied stress was reduced to 0.1 Pa to access low shear rates capable of expanding the steady shear results further.

Fig. 4 shows creep compliance plotted against time for each of the guar galactomannan and rice starch mixtures. The effect of particulate inclusions in the guar galactomannan/rice starch mixtures was, primarily, to decrease the creep compliance parameter below that of the pure system. As the amount of filler was increased the creep

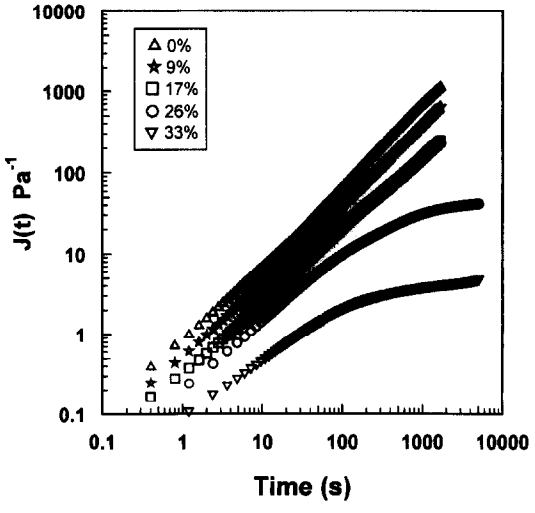

Fig. 4. Effect of increasing rice starch concentration (0–33% w/w) on a double log plot of creep compliance versus time for a 1% guar galactomannan solution.

Table 3. Creep analysis results using automatic steady state determination

Zone	Solvent trap	Stress (Pa)	Viscosity (Pa. s)	Shear rate (s^{-1})	J_o (Pa)	r	Points
0	No	0.5	-9.26×10^4	-5.4×10^{-6}	85.911	−13.01	[a]
0	Yes	0.5	13.418	0.0373	6.090	0.998	180

[a] Steady state was not reached.

compliance ($J(t)$) profiles became more linear with time and on the log time scale appear to 'flatten off'. This is characteristic of a more solid-like system. The most pronounced effect produced by the inclusion of particulate material occurred between the concentrations 17% and 26% (w/w). Here the flow curve changes from increasing at a constant rate with time to an asymptotic 'linear' limit. This can be displayed more clearly using a novel procedure namely by plotting apparent viscosity (Eq. (3)), as calculated in the creep analysis software, versus the reciprocal of time (Fig. 5).

$$\eta_{app} \approx t/J(t) \tag{3}$$

The viscosity–shear rate data displayed in Fig. 2 are incorporated into the same figure along with the new creep data. Likewise, at higher filler concentrations, a power-law behaviour is displayed at low shear rates. The creep experiment has effectively extended the viscosity–shear rate information obtained in the steady shear experiment to two decades lower. However, at very low shear rates, the data points do appear to flatten off for the 33% (w/w) sample. Clearly the scatter here is rather high and we cannot deduce anything substantial from this. The comparison of this effect to a 'pseudo-Newtonian plateau' is uncertain, but the extension of viscosity–shear rate data to such low shear rate regimes has provided some interesting additional information. It is important to appreciate that this

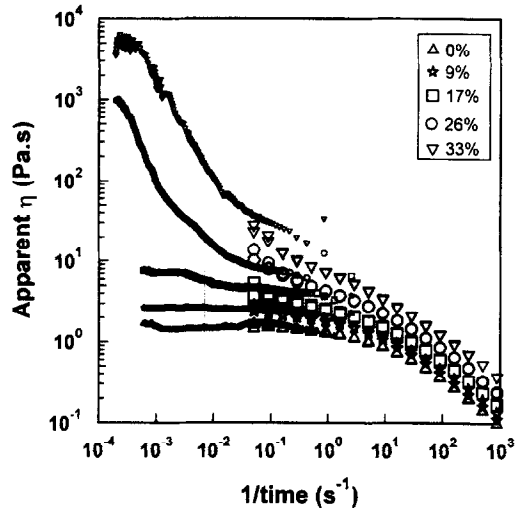

Fig. 5. Effect of increasing rice starch concentration (0–33% w/w) on a double log plot of apparent viscosity versus $1/t$ for a 1% guar galactomannan solution. Steady shear data reproduced from Rayment et al. (1995) is incorporated onto the same graph.

superposition does not include the (geometric) shift to convert the $1/t$ scale to shear rate; the superposition presumably works because this (undetermined and not constant factor[2]) must be of order unity.

Fitting of creep data

The creep compliance data can also be displayed on a graph with the steady shear data. The steady shear data were previously fitted by the yield stress modified Cross equation and the creep compliance viscosity–shear rate data was then simply superimposed on the same graph (Fig. 6(a)). The diagonal clustering of the creep data is partly a feature of plotting the data in this particular manner. Since the dependent variable is the stress level (τ), and strain (γ) is measured as a function of time, we are plotting $\eta = \tau/\dot{\gamma}(t)$ versus $\dot{\gamma}(t) = \gamma(t)/t$. In other words, since τ is constant for a given experiment, we are plotting-log $\dot{\gamma}(t)$ versus log $\dot{\gamma}$(t) − log t. Such a plot must have a slope of −1, and appear to conform with a model, which at long times and low shear rates reduces to $\eta \approx \tau_X/\dot{\gamma} \approx \tau_X t/\gamma$. Nevertheless, it is critical to assert that the absolute positioning of this cluster in $\eta(\dot{\gamma})$ space is not constrained simply by algebra. As described earlier, the model parameters were fitted to the modified Cross model in Fig. P for Windows. In the fit conditions in Fig. P it is possible to adjust the weighting exponent between 0 and 2. This exponent was altered in an attempt to incorporate the creep compliance data in the 95% confidence interval bands of the steady shear data. This appeared to affect the fit only at the high shear rate end of the plot and, therefore, was not an advantage in this case. Fig. 6(b) shows the same data fitted with a weight exponent of zero. A very slight widening can be seen in the interval bands at shear rates close to 1000 s^{-1} and also at low shear rates, if the confidence interval is increased.

Fig. 7 shows the creep and steady shear data plotted in the same way for all the guar galactomannan/rice starch mixtures. The controlled (constant) stress data appear as a diagonal cluster with a slope of −1, as would be expected from the power-law equation and from previous discussion. Although previously the creep compliance data was displayed with the steady shear data fitted to the modified Cross equation, attempts were made to also fit just the creep data to the same model. Firstly, the creep compliance zone 4 data were incorporated with the steady shear

[2] Since the stress (rate) is being controlled rather than the strain rate.

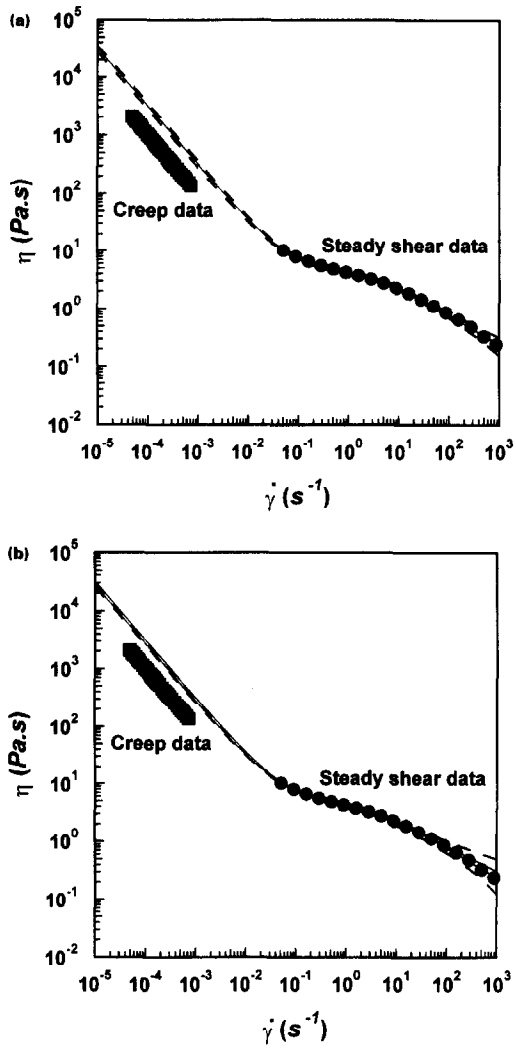

Fig. 6. (a) Viscosity–shear rate profile for a 1% guar galactomannan/26% rice starch mixture. The steady shear viscosity–shear rate data is fitted to the modified Cross equation with the creep compliance data superimposed on the same graph. Dotted lines represent 95% confidence limits. Weight exponent = 2. (b) Data as (a) but with weight exponent = 0.

viscosity–shear rate data and then fitted to the yield stress modified Cross equation using the Simplex least-squares fitting method. The results are listed in Table 4. Least squares fitting to the model was then carried out using the Marquardt algorithm in Fig. P. This was identical with that used with the steady shear data.

The parameter a (in Eq. (2)), which represents a relaxation time, increased as the filler concentration increased. The exponent p decreased as filler concentration increased. As we would predict from Eq. (2), when the filler volume fraction was increased the power-law behaviour is more pronounced and p tended to -1. Further investigation showed that even when using two points of the creep compliance data (first and last values) with the steady shear data, the parameters calculated in Fig. P were significantly affected. Table 5 shows the parameters calculated using the yield stress modified Cross equation for the zone 4

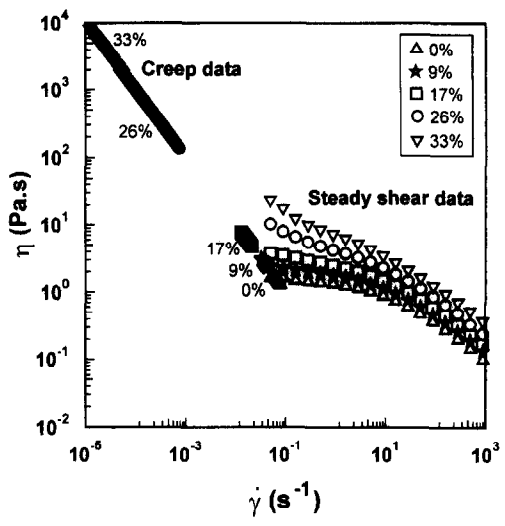

Fig. 7. Graph to show the steady shear viscosity–shear rate data for a 1% guar galactomannan solution filled with rice starch (0–33% w/w) fitted to the modified Cross equation with creep compliance data superimposed on the same graph.

creep data (50 points) and two points of this data with the steady shear data. Fig. 8 shows the least-squares fitting of the data in Fig. P with two points of the creep data.

Attempts were made to fit the creep data (only) to the modified Cross model. However, due to the low shear rates accessed, the $\tau/\dot{\gamma}$ term in the modified Cross equation tends to a large value. This means that at higher filler concentrations the shear rate is reduced further and the yield stress term increases. The model tendency is to return the 'yield stress' fit parameter as exactly the shear stress applied. This reflects the weighting effect mentioned earlier. The problem appears to be that the model is not suitable to analyse large amounts of data (50 points) which occur as a diagonal cluster at low shear rates.

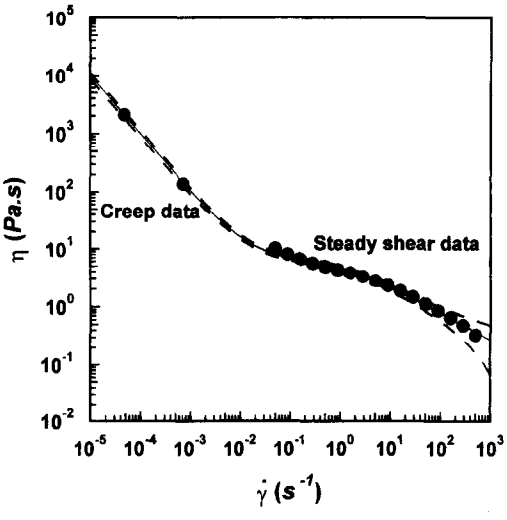

Fig. 8. Graph to show the steady shear data and two points of the creep data fitted in Fig. P for a 1% guar galactomannan/26% rice starch mixture. Dotted lines represent 95% confidence limits.

Table 4. Creep compliance test data (zone 4 only) and steady shear data fitted to the modified Cross equation

Filler (%)	Zero-shear viscosity (Pa. s)	Yield stress (Pa)	*a* (s)	*p*	Sum of squares ($\times 10^{-2}$)
0	1.3354	0.0135	0.0449	0.6927	6.541
0	1.3870	0.0073	0.0506	0.6790	4.909
0	1.3917	0.0117	0.0514	0.6768	4.089
9	1.9889	0.0292	0.0719	0.6343	1.865
9	1.9173	0.0307	0.0633	0.6473	3.716
9	2.1013	0.0225	0.0869	0.6166	1.134
17	3.0109	0.0464	0.1142	0.6149	1.483
17	2.9152	0.0597	0.1030	0.6228	1.256
17	2.9722	0.0599	0.1105	0.6164	2.994
26	7.7118	0.0986	0.6111	0.5339	1.515
26	7.7309	0.0984	0.6166	0.5334	1.483
26	7.7603	0.0985	0.6258	0.5327	1.405
33	29.7670	0.0994	10.3910	0.4652	2.704
33	29.7182	0.0995	10.3325	0.4654	2.704
33	29.7087	0.0992	10.3196	0.4654	2.714

Table 5. Calculated modified Cross equation parameters using all steady shear data alone (0 points) plus 50 and two points of the creep data, respectively

Points used	Filler (%)	Zero-shear viscosity (Pa. s)	Yield stress (Pa)	*a* (s)	*p*	Sum of squares
0	26	5.3368	0.2678	0.1871	0.5948	7.064×10^{-4}
50	26	7.7118	0.0986	0.6111	0.5339	1.515×10^{-2}
2	26	10.5270	0.0948	2.1348	0.4732	1.863×10^{-2}

Further experiments were carried out to determine the effect of applied stress on a 1% guar galactomannan/33% rice starch mixture. The results were plotted with the steady shear viscosity–shear rate data for the same filler concentration (Fig. 9). The steady shear data had previously been fitted by the yield stress modified Cross equation. The creep data superimposes closely with the steady shear data at high stresses, whilst at stresses of 0.5 Pa and below, the data deviates from the modified Cross fit.

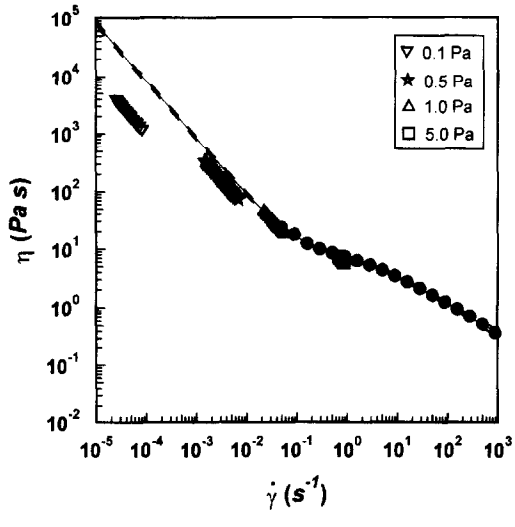

Fig. 9. Graph to show the steady shear viscosity–shear rate data fitted to the modified Cross equation with creep compliance data superimposed for 1% guar galactomannan/33% rice starch mixture. Creep data determined at different command stresses (0.1–5.0 Pa). Dotted lines represent 95% confidence limits.

The yield stress parameter in the equation was fixed at each applied stress (0.1, 0.5, 1.0 and 5.0 Pa) and the results are displayed in Table 6. The calculated zero-shear viscosity for the unfixed yield stress parameter lies somewhere between the values at 0.5 and 1.0 Pa fixed yield stress. This is as expected since the unconstrained yield stress value is 0.834 Pa. The viscosity parameter was then fixed in turn at values between 1.0 and 50.0 Pa. s. The overall data appear best fitted when the viscosity and yield stress terms are fixed at 10 Pa. s and 1 Pa, respectively (Fig. 10). As expected, these values are close to the values determined for the unconstrained data in Fig. P (7.4 Pa. s and 0.8 Pa).

DISCUSSION

In this paper a number of creep experiments have been undertaken on a starch filled guar solution with resulting test parameters calculated. These appear to depend on the attainment of a steady state within the duration of the test. More problems were encountered with the heavily filled systems in which solid-like properties are of paramount importance. Creep measurements allow investigations at very low shear rates which are critical in the study of

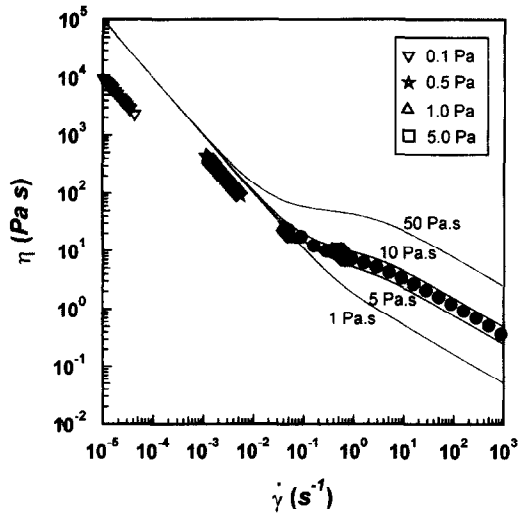

Fig. 10. Data as Fig. 9 but steady shear data fitted to modified Cross equation with fixed yield stress parameter of 1.0 Pa. Lines represent fixed viscosity term of 1, 5, 10 and 50 Pa. s, respectively.

these systems. The existence of a yield stress can be investigated with particular emphasis on confirmation of the data previously obtained in steady shear (Rayment et al., 1995). A yield stress is the critical stress below which no flow is recorded. This depends strongly on the experimental design and accuracy of the rheometer, although it can be stated that all materials will flow during some finite time scale (Barnes and Walters, 1985; Husband *et al.*, 1993).

A number of rheological parameters have been studied including creep compliance ($J(t)$), instantaneous compliance (J_0), zero-shear viscosity (η_0) and yield stress (τ_X), to investigate the effect of particulate inclusions on a guar galactomannan solution. The creep compliance parameter has decreased with increasing filler and since creep compliance is the reciprocal of modulus in dynamic measurements, this is indicative of a more solid-like behaviour. The filler serves to reinforce the guar galactomannan network and increase the longest relaxation time of the system. By increasing filler concentration the effect on the creep compliance–time profile was considerable (Fig. 4). The position and shape of the curves were strongly influenced. The effect of increasing filler concentration is, primarily, to reduce the creep compliance parameter below that of the pure system and to make it more linear with respect to time. This is characteristic of more solid-like properties in the system. Shear strain becomes constant with time and therefore, at a constant stress, compliance becomes linear also (Hookean response).

The zero-shear viscosity and apparent yield stress results obtained in steady shear have previously been fitted to a master curve relating these parameters to volume fraction (Rayment *et al.*, 1995). The normalised zero-shear viscosity increased significantly as the filler concentration approaches the maximum packing fraction of the system. In the earlier publication by Rayment *et al.* (1995), we assumed that

Table 6. Least-squares fitting of steady shear viscosity–shear rate data to the modified Cross equation. Calculated parameters with yield stress value in model fixed and unfixed

Yield stress (Pa)	Zero-shear viscosity (Pa. s)	a (s)	p
0.834 [a]	7.410	0.4153	0.4985
0.1	17.915	6.7889	0.4273
0.5	9.735	0.9677	0.4712
1.0	6.637	0.2987	0.5105
5.0	1.108	0.0004	1.0000

[a] Yield stress parameter unconstrained (limit $0 < p$).

zero-shear viscosity tends towards infinity and became too large to measure at a certain critical concentration. The occurrence of a yield stress on increasing filler concentration appeared to be more gradual and the data tended to fit a straight line equation where $\log(\tau_X) \propto \phi$. Now, the new creep data clearly support the evidence that there is an apparent upswing in the steady shear viscosity–shear rate data at low shear rates (Fig. 7), which had previously been deduced only from a few data points at the lowest accessible steady shear rate. However, problems were encountered when trying to fit this data to the modified Cross model. In data fitting terms, the model was 'overdetermined', i.e. there are too many parameters for the functional form of the data. In practice this type of data would be better analysed using a power-law type equation. Poslinski *et al.* (1988) used this approach in their study of filled polymeric systems exhibiting apparent yield stress. The Bird–Carreau model (Bird and Carreau, 1968) was used to describe data obtained from an unfilled high molecular weight thermoplastic polymer and a power law equation to describe this system filled with ceramic particulates. Overall, we need the full form of the equation for data measured at $\dot{\gamma} \geq 1\ s^{-1}$, at lower values, and at high filler volume fractions, a simple power-law probably works just as well.

CONCLUSION

The importance of experiments at low shear rates have been established with particular emphasis on the comparison with and expansion of steady shear data. The presence of an apparent yield stress in the filled systems appears to be firmly supported by the experiments described in this paper. Moreover, it does appear that the yield stress modified Cross equation best describes an aqueous dispersion of guar galactomannan with 5–25% filler. However, for systems above and below this regime a power law and Cross type model, respectively, would fit better. The yield stress modified Cross equation should, nevertheless, prove useful in describing systems of a particulate concentration encountered in real food systems, and future work should concentrate on the effect of particle size and shape (and their distribution).

ACKNOWLEDGEMENTS

PR acknowledges the receipt of a Ministry of Agriculture, Fisheries and Food studentship and Leatherhead Food Research Association for their collaboration and financial support. The authors also acknowledge the support of BBSRC for the purchase of the Rheometrics Fluids Spectrometer (F01033) and, more recently, the Dynamic Stress Rheometer (F06419). We are grateful to Professor Iain Dea of Quest International, Naarden, The Netherlands for helpful discussions.

REFERENCES

Barnes, H.A., Walters, K. (1985) The yield stress myth?. *Rheologica Acta*, **24**, 323–326.

Bird, R.B., Carreau, P.J. (1968) A nonlinear viscoelastic model for polymer solutions and melts—I. *Chem. Eng. Sci.*, **23**, 427–434.

Castelain, C., Lefebvre, J., Doublier, J. L (1986) Rheological behaviour of BSA–cellulose derivative mixtures in neutral aqueous medium. *Food Hydrocolloids*, **1**, 141–151.

Cross, M.M. (1965) Rheology of non-Newtonian fluids: a new flow equation for pseudoplastic systems. *J. Colloid Science*, **20**, 417–437.

Dea, I.C.M., Morrison, A. (1975) Chemistry and interactions of seed galactomannans. *Adv. Carb. Chem. Biochem.*, **31**, 241–312.

Doublier, J.L., Launay, B. (1981) Rheology of galactomannan solutions: comparative study of guar gum and locust bean gum. *J. Texture Studies*, **12**, 151–172.

Husband, D.M., Aksel, N., Gleissle, W. (1993) The existence of static yield stress in suspensions containing non colloidal particles. *J. Rheol.*, **37**(2), 215–235.

Lapasin, R., Pricl, S. (1995). *Rheology of Industrial Polysaccharides—Theory and Applications*. London: Blackie Academic and Professional.

Poslinski, A.J., Ryan, M.E., Gupta, R.K., Seshadri, S.G., Frechette, F.J. (1988) Rheological behaviour of filled polymeric systems, I. Yield stress and shear-thinning effects. *J. Rheol.*, **32**(7), 703–735.

Rayment, P.R., Ross-Murphy, S.B., Ellis, P.R. (1995) Rheological properties of guar galactomannan and rice starch mixtures—I. Steady shear measurements. *Carbohydr. Polym.*, **28**, 121–130.

Richardson, R.K., Ross-Murphy, S.B. (1987) Non-linear viscoelasticity of polysaccharide solutions. 1: Guar galactomannan solutions. *Int. J. Biol. Macromol.*, **9**(5), 249–312.

Robinson, G., Ross-Murphy, S.B., Morris, E.R. (1982) Viscosity–molecular weight relationships, intrinsic chain flexibility, and dynamic solution properties of guar galactomannan. *Carbohydr. Res.*, **107**, 17–32.

Rutgers, Ir.R. (1962) Relative viscosity of suspensions of rigid spheres in Newtonian liquids. *Rheologica Acta*, **2**(3), 202–210.

Sharman, W.R., Richards, E.L., Malcolm, G.N. (1978) Hydrodynamic properties of aqueous solutions of galactomannans. *Biopolymers*, **17**, 2817–2833.